Letters on Materials 12 (2), 2022 pp. 142-147 www.lettersonmaterials.com

https://doi.org/10.22226/2410-3535-2022-2-142-147

Improving the accuracy of finite element modeling of superplastic forming processes

O. Tulupova[†,1], C. Gumerova[1], V. Ganieva[1], A. Kruglov[2], F. Enikeev[1]

[†]box_mail_2011@mail.ru

[1]Ufa State Petroleum Technological University, Ufa, 450064, Russia
[2]Institute for Metals Superplasticity Problems, RAS, Ufa, 450001, Russia

A method of improving the accuracy of finite element modeling of superplastic forming processes is suggested. It is based on improving the accuracy of determining the values of material constants for the standard power law of superplastic flow from the results of technological experiments under constant pressure forming of hemispherical domes. Unlike other known procedures, the method suggested takes into consideration the initial stage of superplastic forming, when the pressure of the inert gas changes from the initial zero level to a pre-given constant value. Since this part of loading is usually neglected in reports known in the literature the main attention in the present study is paid to the analysis of its importance as far as the accuracy of finite element modeling is concerned. Besides, the entry radius in the die used is also a variable in the analysis. The calculations are performed for alloys Ti-6Al-4V, AZ31, AA5083 using the experimental data known in the literature. Finite element modeling is carried out using the ANSYS code. It is concluded that the influence of the initial part of loading should be considered in finite element modeling of the superplastic forming processes since this factor can affect the accuracy of predictions.

Keywords: superplastic material, superplastic forming, modeling, material constants, finite element modeling.

1. Introduction

The pioneering work of Backofen et al. [1] commenced a new era in studying superplastic flow. As a result, thousands of reports have been reported in the literature where the superplastic forming of a sheet material into a cylindrical die has been considered from various points of view. The most important characteristic of the superplastic flow is believed to be the value of the material constant m for the standard power law of superplasticity $\sigma = K\xi^m$, where σ is the flow stress, ξ is the strain rate and K is a material parameter, which depends on the temperature and microstructure of the material to be deformed. Various procedures to determine the value of m from the uniaxial mechanical experiments have been developed [2]. Some simplified models of superplastic forming of dome into a cylindrical die have been proposed, see, e. g., [3–6]. Methods are also available to determine the value of material constant m [6–11]. The common scheme to do it is described in [11] and later extended in [12].

Since the classic works of Jovane [3], Cornfield and Johnson [4], Holt [5] and others the initial (transient/unsteady) stage of forming has not been taken into consideration when analysing the constant pressure forming of domes. However, it is clear the constant pressure cannot be applied to the sheet instantaneously. Some time is required to achieve the value of pressure selected. The influence of this region on the overall deformation process is unclear. The aim of the present report is to critically examine this problem, i. e., to understand, if it is possible to neglect the initial transient stage of forming or should it be taken into consideration. To answer this question, a quantitative analysis is carried out with the aim of obtaining numerical estimations of the errors additionally introduced due to a neglect of the presence of the initial unsteady state of forming.

2. Fundamentals

One can find below the extension of the former analysis reported in [6], the initial part of loading along with entry radius of the die set used being taken into consideration in the analysis.

2.1. Simplified approach

Let us consider the deforming of a thin sheet of initial thickness s_0 into a cylindrical die of radius R_0 having non-zero entry radius r_0 as shown in Fig. 1.

The simplified approach to the analysis of the process of superplastic forming of a sheet into a cylindrical die has been suggested in [6] where no initial stage of superplastic forming and entry radius have been taken into consideration.

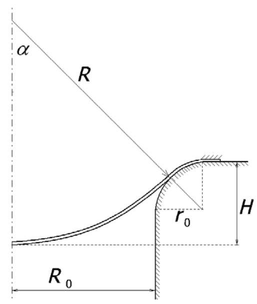

Fig. 1. Schematic of deforming a sheet into a cylindrical die.

Later this approach was extended with the aim to include the presence of non-zero entry radius [13]. It is used below to study the influence of the initial stage of superplastic forming.

The free sliding of a sheet along the die is assumed in further analysis keeping in mind that a good lubricant is used in practice in a forming experiment. Assuming the free part of the shell to be a part of a sphere of radius R one can conclude that the length of every meridian passing the dome apex is equaled to $(R+r_0)\alpha$, where α is the angle between the axis of symmetry and radius of this sphere passing the center of curvature of the entry radius (see Fig. 1). As the initial length of the meridian is equal to (R_0+r_0), one can conclude that every meridian passing the dome apex is stretched as $[(R+r_0)\alpha/(R_0+r_0)]$. In view of the geometric relation $[R_0+r_0=(R+r_0)\sin\alpha]$ one can derive the following relation for the thickness of the shell at the dome apex: $s_a=s_0[(R+r_0)\alpha/(R_0+r_0)]^2=s_0(\sin\alpha/\alpha)^2$.

It is noted that a similar relation has been reported earlier in [6] where no entry radius was included. Consequently, the strain rate at the dome apex, ξ_{ea}, is given by: $\xi_{ea}=2\xi m=2(d\alpha/dt)\cdot(1/\alpha-\text{ctg}\,\alpha)$.

In accordance with standard assumptions of thin shell theory, the stress state is assumed to be described by two non-zero components of stress: meridian stress, σ_m, and tangential stress, σ_t. Then one can derive for the dome apex the following relations: $\sigma_e=\sigma_m=\sigma_t=pR/2s$, where σ_e is equivalent Mises stress, s is the current thickness of the shell and p is the inertial pressure of the gas supplied. It follows, therefore, that the following relations are valid at the dome apex: $\sigma_{ea}=pR/2s_a=p[(R_0+r_0)/2s_0]\cdot[1-r_0\sin\alpha/(R_0+r_0)]\cdot\alpha^2/\sin^3\alpha$.

The standard power law of superplasticity $\sigma=K\xi^m$ is chosen to represent the material response. Here σ is flow stress, ξ is strain rate while K and m are material constants to be determined experimentally. For multiaxial loading the standard power law of superplasticity can be written as $\sigma_{ea}=K\xi_{ea}^{\ m}$ where σ_{ea} is the Mises equivalent stress at the dome apex. Then, one can derive the following expression: $\sigma_{ea}=p[(R_0+r_0)/2s_0]\cdot[1-r_0\sin\alpha/(R_0+r_0)]\cdot\alpha^2/\sin^3\alpha=K[2(d\alpha/dt)\times(1/\alpha-\text{ctg}\,\alpha)]^m$.

This relation represents an ordinary differential equation with respect to the unknown function $\alpha=\alpha(t)$ which may be rewritten as follows: $2\{\sin^3\alpha/\alpha^2/[1-r_0\sin\alpha/(R_0+r_0)]\}^n\times(1/\alpha-\text{ctg}\,\alpha)d\alpha/dt=[(R_0+r_0)/2Ks_0]^n p^n$, where $n=1/m$ and pressure p, in general, is a function of time t.

Particular solution of this differential equation satisfying the initial condition $\alpha(0)=0$ can be written as follows: $[(R_0+r_0)/2Ks_0]^n\int[p(\tau)]^n dt=2I'_m(\alpha)$, where the function $p(\tau)$, $0\le\tau\le t$ describes the pressure-time cycle while I'_m is the following special function of two variables, m and α, viz., $I'_m(\alpha)=\int\{\sin^3x/x^2/[1-r_0\cdot\sin x/(R_0+r_0)]\}^n\cdot(1/x-\text{ctg}\,x)dx$, where the integration is from 0 to α.

In order to obtain the time dependence of the dome height, H, the following geometric relations may be used: $H(t)=R-R\cos\alpha+r_0-r_0\cos\alpha=(R_0+r_0)\cdot\text{tg}(\alpha/2)$, when $R_0+r_0\approx\approx(R+r_0)\sin\alpha$.

To estimate the influence of contact friction on the results, it is reasonable to consider the alternative limiting condition of sticking friction. Let us consider two consecutive strain states as shown in Fig. 2. Here, A is the dome apex, B corresponds to the boundary of the deforming zone, C belongs to the interface between two parts of deforming shell having different curvatures: AC has a curvature R_0, while BC a curvature r_0.

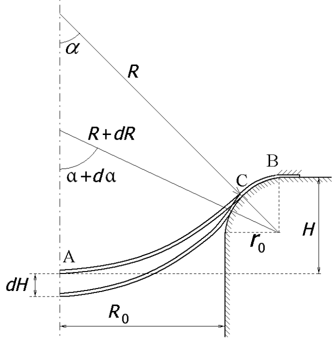

Fig. 2. Two consecutive steps of forming.

During forming the part AC sticks to the die and so this part no longer deforms during further processing. Therefore, the increment in meridian strain, $d\varepsilon_m=d(\text{AC})/\text{AC}$, is then given by: $d\varepsilon_m=[(R+dR)\cdot(\alpha+d\alpha)+r_0d\alpha-R\alpha]/(R\alpha)=dR/R+(1+r_0/R)d\alpha/\alpha$.

From the geometric relation $(R+r_0)\sin\alpha=R_0+r_0$, the following expression can be derived for the meridian strain rate: $\xi_m=d\varepsilon_m/dt=(d\alpha/dt)\cdot(1/\alpha-\text{ctg}\,\alpha)/(1-r'_0\cdot\sin\alpha)$ (sticking), where $r'_0=r_0/(R_0+r_0)$ is a dimensionless geometric parameter characterizing the entry radius. Evidently, $0\le r'_0\le 0.5$.

Biaxial strain takes place at the dome apex so that the principal logarithmic strains at the pole may be obtained as: $\varepsilon_m=\varepsilon_t=\int d\varepsilon_m dt$.

From the incompressibility condition $\varepsilon_m+\varepsilon_t+\varepsilon_n=0$ and $\varepsilon_n=\ln(s_a/s_0)$. So, it follows that $\ln(s_a/s_0)=-2\int d\varepsilon_m dt$ and consequently $\ln(s_a/s_0)=2\int d\varepsilon_m dt=2\int(1/x-\text{ctg}x)/(1-r'_0\cdot\sin x)dx$ where the integration is from 0 to α.

As a result, the thickness of the shell at the dome apex when sticking friction is present is: $s_a=s_0\cdot\exp\{-2\int(1/x-\text{ctg}\,x)/(1-r'_0\cdot\sin x)dx\}$ where the limits of integration are from 0 to α. This expression is not convenient for practical applications and so an approximation is recommended for practical applications where numerical computations are involved, viz.,

$$s_a=s_0\cdot\exp\left[\frac{2\cdot\ln\left(\dfrac{\sin\alpha}{\alpha}\right)}{1-0.825\cdot r'_0\cdot\sin\alpha}\right]. \tag{1}$$

The deviation of this approximate solution from the exact one when $0\le r'_0\le 0.5$ is not more than 4%, while for the more reasonable diaphragm $0\le r'_0\le 0.15$, the deviation is less then 0.1%.

Following the same procedure, for sliding friction the following differential equation can be derived:

$$\sigma_e=p\cdot\left[\frac{R_0+r_0}{2s_0}\right]\cdot\left[1-r'_0\sin\alpha\right]\cdot\frac{1}{\sin\alpha}\cdot\exp\left[\frac{-2\ln\left(\dfrac{\sin\alpha}{\alpha}\right)}{1-0.825\cdot r'_0\sin\alpha}\right]=$$

$$=K\xi_e^m=K\left[\frac{2\dfrac{d\alpha}{dt}\cdot\left(\dfrac{1}{\alpha}-\text{ctg}\alpha\right)}{1-r'_0\sin\alpha}\right]^m. \tag{2}$$

2.2. Constant pressure loading

To calculate the time dependence α(t) for the case of constant pressure loading $p=p_0=$constant, the principal differential equation derived above can be rewritten as: $t\cdot[p_0\cdot(R_0+r_0)/2Ks_0]^n=2I'_m(\alpha)$.

From this, it follows that the value of the material constant, m, can be determined from the results of two constant pressure forming experiments as follows: $m=\ln(p_2/p_1)/\ln(t_1/t_2)$, where t_1 and t_2 are the duration of forming of a sheet material to same dome height, H, under constant pressures $p=p_1=$constant and $p=p_2=$constant, respectively, i.e. $H(t_1)=H(t_2)$.

The value of the second material constant, K, is determined using the following equations:

$$K_1=\frac{p_1(R_0+r_0)}{2s_0}\cdot\left[\frac{t_1}{2I'_m(\alpha)}\right]^m, \tag{3}$$

$$K_2=\frac{p_2(R_0+r_0)}{2s_0}\cdot\left[\frac{t_2}{2I'_m(\alpha)}\right]^m. \tag{4}$$

The mean value can then be calculated as $K=(K_1+K_2)/2$.

Thus, to determine the values of material constants, K, m, it is enough to carry out two constant pressure forming experiments under different constant pressures p_1, p_2 to the same dome height $H(t_1)=H(t_2)$. In principle, constant pressure forming to different dome heights $H(t_1)\neq H(t_2)$ can also be used to determine the values of K, m, but that case will be considered elsewhere.

2.3. Linear pressure law

Let us consider the following regime of loading as shown in Fig. 3.

As can be seen from Fig. 3, pressure linearly increases in the first stage (when $t<t_0$) in accordance with the rule $p(t)=p_{0t}/t_0$ beyond which (i.e., when $t>t_0$) constant pressure loading takes place at $p=p_0=$constant. In this case, the principal differential equation derived above may be written as follows.

$$\left[\frac{R_0+r_0}{2Ks_0}\right]^{1/m}\cdot\int[p(\tau)]^n\,dt= \\ =\left[\frac{R_0+r_0}{2Ks_0}\right]^{1/m}\cdot\left(\frac{p_0}{t_0}\right)^{1/m}\cdot\left[\frac{m}{m+1}\right]\cdot t^{1+1/m}=2I'_m(\alpha), \tag{5}$$

$$t=\left(\frac{2Ks_0t_0}{p_0(R_0+r_0)}\right)^{1/(m+1)}\cdot\left[\left(1+\frac{1}{m}\right)\cdot 2I'_m(\alpha)\right]^{m/(m+1)}. \tag{6}$$

When $t=t_0$, the value of angle α_0 is determined as follows: $t_0=[(m+1)/m]\cdot[2Ks_0/p_0(R_0+r_0)]^{1/m}\cdot 2I'_m(\alpha_0)=(1+1/m)t_{f0}$, where t_{f0} is the duration of forming to the angle α_0 (dome's height $H=H_0=(R_0+r_0)\mathrm{tg}(\alpha_0/2)$) under constant pressure $p=p_0=$constant. Thus, the duration of forming to the arbitrary dome height $H=H_0=(R_0+r_0)\mathrm{tg}(\alpha_0/2)(0<\alpha<\pi/2)$ under linear pressure law is $(1+1/m)$ times larger as compared to the duration of forming under constant pressure equal to the value of pressure at the end of forming (i.e. under $p=p_0=$constant).

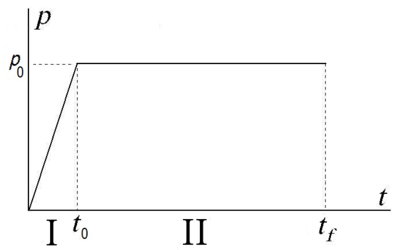

Fig. 3. Schematic of the pressure-time cycle.

Now, the following procedure can be suggested to determine the values of the material constants, K and m, from the results of two technological experiments corresponding to two stages: linear pressure law up to some intermediate time t_0 and constant pressure forming when $t_0<t<t_f$. Let us assume that during two independent technological experiments the following data have been recorded: initial stages t_{01} and t_{02}, total forming time t_{f1} and t_{f2}, pressure p_1 and p_2.

From the results of the above analysis, one can conclude that for constant pressure forming the following relations are valid: $t_1=t_{01}/(1+1/m)+\Delta t_1$ and $t_2=t_{02}/(1+1/m)+\Delta t_2$, where $\Delta t_1=t_{f1}-t_{01}$ and $\Delta t_2=t_{f2}-t_{02}$. From this it follows that the value of the material constant, m, can be estimated from

$$m=\frac{\ln(p_2/p_1)}{\ln(t_1/t_2)}=\frac{\ln(p_2/p_1)}{\ln\left(\dfrac{t_{01}/(1+1/m)+\Delta t_1}{t_{02}/(1+1/m)+\Delta t_2}\right)}.$$

This is a transcendental equation with respect to the unknown value of m which can be solved by a suitable numerical method.

3. Approbation of the procedure suggested

The following minimum set of experimental data are sufficient to complete the calculations: {t, p, s, H, t_0}, where t is the total forming time of a shell; p is the gas pressure; H is the height of the dome; s is the thickness of the dome at the dome apex; t_0 is the duration of the first stage of forming (when the pressure linearly increases from an initial value of zero to a pre-selected value, p). Two different sets of the experimental data known in the literature have been used for the calculations.

Table 1 includes the results of superplastic forming of titanium alloy Ti-6Al-4V [14]. A sheet of initial thickness 1 mm was formed into a cylindrical die having a radius 35 mm and entry radius 1 mm. The following notations are used in Table 1: i is the number of the forming experiment; t_f is the total time of forming; t_{0i} is the duration of the first stage of forming.

Tables 2 and 3 include experimental data from [7,8] obtained by the blow forming of hemispheres of magnesium alloy AZ31 and aluminum alloy AA5083. In these works [7,8], the time of unsteady pressure supply is not considered. Therefore, in the analysis this value was equated to zero. In the case of magnesium alloy AZ31, a sheet of initial thickness 0.5 mm was formed into a cylindrical die of radius 35 mm and an entry radius 3 mm [7]. The sheet aluminum alloy AA5083

Table 1. Experimental data on superplastic forming of Ti-6Al-4V alloy [14].

№	Temperature of SPF	Gas pressure	Total time	Initial stage	Forming time	Height of the hemisphere
i	T, °C	p, MPa	t_{fi}, s	t_{0i}, s	t, s	H, mm
1	750	3	360	55	305	35
2	750	2.5	510	40	470	35

Table 2. Experimental data on superplastic forming of AZ31 magnesium alloy [7].

№	Temperature of SPF	Gas pressure	Forming time	Height of the hemisphere
i	T, °C	p, MPa	t, s	H, mm
1	519.85	0.16	782.0	20.4
2	519.85	0.29	183.0	18.7

Table 3. Experimental data on superplastic forming of AA5083 aluminum alloy [8].

№	Temperature of SPF	Gas pressure	Forming time	Height of the hemisphere
i	T, °C	p, MPa	t, s	H, mm
1	450	0.29	1080.0	46.5
2	450	0.56	120.0	43.2

of initial thickness 1.2 mm was formed into a cylindrical die of radius 50 mm and an entry radius 5 mm [8].

Experimental data listed in Tables 1, 2 and 3 were analyzed in accordance with the procedure outlined above. The results are collated in Table 4 for use in the subsequent finite element analysis using ANSYS software.

4. Finite element modeling

Comparison of the results of calculations based on analytical formulas appears to be not enough to make a substantiated conclusion concerning the validity of a procedure suggested. That is why, finite element modeling of the process of superplastic forming of a hemisphere is considered to be pertinent in this connection. One can find many reports in the literature devoted to finite element analysis of superplastic forming of domes using finite element codes like ANSYS [16–19] and ABAQUS [20,21]. In this study, the educational version of ANSYS 10ED program was used. The boundary value problem in the mechanics of solids was stated in terms of the theory of creep using standard power law of superplasticity, as described, e.g., in [15].

To solve the boundary value problem, the values of material constants m and K were used as input data (see Table 4).

Finite element mesh used is shown in Fig. 4, where R_0 is die radius, r_0 is entry radius, s_0 is initial thickness and H is dome height.

Finite element mesh includes 4 layers consisting of 990 8-nodes elements PLANE183 (Fig. 5).

Contact interaction of the sheet with the die is modeled using contact pair of elements CONTA172 and TARGET169. The part of mesh in the vicinity of entry radius is shown in Fig. 6.

The results of finite element modeling of the duration of forming Structural/ANSYS hemispheres from different alloys at different pressures are summarized in Tables 5, 6 and 7.

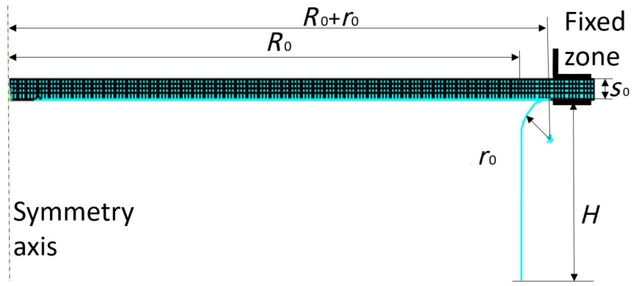

Fig. 4. (Color online) Finite element mesh.

Tables 5, 6 and 7 reveal that the results of finite element calculations are close to the experimental results. For example, for Ti-6Al-4V alloy, assuming the calculated values of material constants $m = 0.451$, $K = 1454.035$ MPa·s^m, one obtains the forming time in ANSYS (when solving the boundary value problem of creep theory) of 359.6 s and 513.6 s, respectively, i.e., the deviation from the experimental values does not exceed 1% (see Table 5). In contrast, if the initial stage of forming (when the pressure increases from zero to a pre-selected value) is not taken into consideration, the deviation is about 2.6%.

For the AZ31 alloy, using values $m = 0.409$, $K = 174.664$ MPa·s^m in ANSYS, the forming time is 800.8 s and 186.5 s, respectively, i.e., the deviation from the experimental values does not exceed 3% (see Table 6).

The increase in the percentage of deviation of numerical results from experimental values from 1% to 3% is due to the fact that in calculations obtained as a result of experiments on test molds of hemispheres from magnesium and aluminum alloys, the pressure supply time in the first stage was equated to zero, i.e., it was not included in the total time of forming the hemisphere.

Time dependence of the dome height calculated in accordance with the equations derived in the finite element analysis are compared in Fig. 7, 8 and 9.

Table 4. Rheological parameters calculated for Ti-6Al-4V, AZ31 and AA5083 alloys.

	Ti-6Al-4V			AZ31	AA5083
	Considering the varying pressure supply time in the first stage	Not considering the pressure supply time in the first stage	Not considering the pressure supply time in the first stage and the entry radius	Not considering the pressure supply time in the first stage	
m	0.45	0.523	0.52	0.41	0.29
K, MPa·s^m	1454	2364.28	2343.67	174.7	97.92

Table 5. The duration of forming of hemispheres of radius $R_0 = 35$ mm from the Ti-6Al-4V sheets of initial thickness $s_0 = 1$ mm.

Gas pressure, MPa	Forming time, s				Δ, %
	Experimental data	ANSYS			
		Considering the pressure supply time in the first stage	Not considering the pressure supply time in the first stage	Not considering the pressure supply time in the first stage and entry radius	
3	360.0	359.6	369.3	378.5	≈0.1/≈2.6/≈5.1
2.5	510.0	513.6	523.0	536.3	≈0.7/≈2.6/≈5.2

Table 6. The duration of forming of hemispheres of radius $R_0 = 35$ mm from AZ31 sheets of initial thickness $s_0 = 0.5$ mm.

Gas pressure, MPa	Forming time, s		Δ, %
	Experimental data	ANSYS	
0.16	782.0	800.8	≈2.4
0.29	183.0	186.5	≈1.9

Table 7. The duration of forming of hemispheres of radius $R_0 = 50$ mm from AA5083 sheets of initial thickness $s_0 = 1.2$ mm.

Gas pressure, MPa	Forming time, s		Δ, %
	Experimental data	ANSYS	
0.29	1080.0	1061	≈1.8
0.56	120.0	123.5	≈2.9

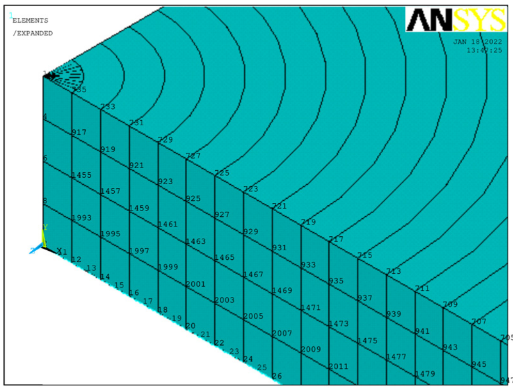

Fig. 5. (Color online) Numbered nodes at the initial moment of time.

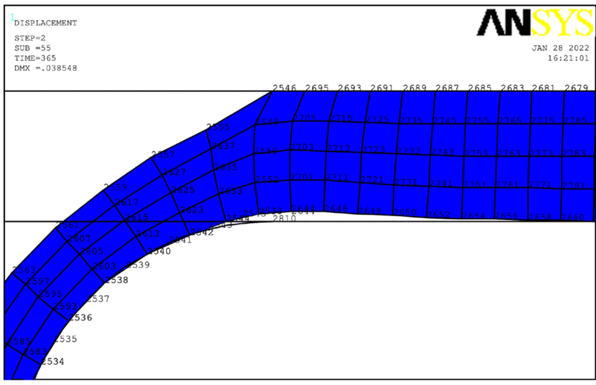

Fig. 6. (Color online) Finite element mesh in 365 seconds.

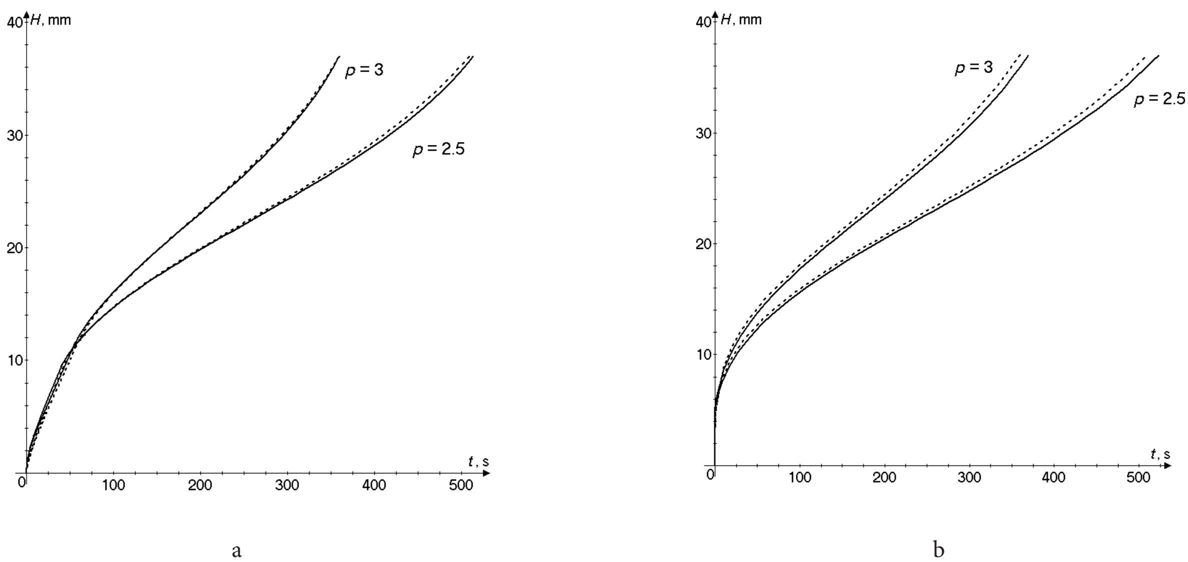

Fig. 7. Time dependence of the dome height H, mm, for titanium alloy Ti-6Al-4V calculated using ANSYS/Structural (solid lines) and by means of simplified analytical solutions considering the pressure supply time in the first stage (dashed lines) under different pressure, MPa, (indicated by the numbers near the curves) with $m = 0.45$, $K = 1454$ MPa·s^m and $m = 0.52$, $K = 2364.3$ MPa·s^m (b).

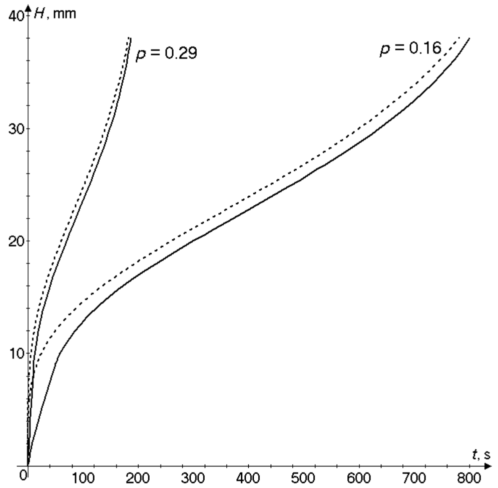

Fig. 8. Time dependence of the dome height *H*, mm, for magnesium alloy AZ31 calculated using ANSYS/Structural (solid lines) and by means of simplified analytical solutions (dashed lines) under different pressure, MPa, (indicated by the numbers near the curves) with $m = 0.41$, $K = 174.7$ MPa·s^m.

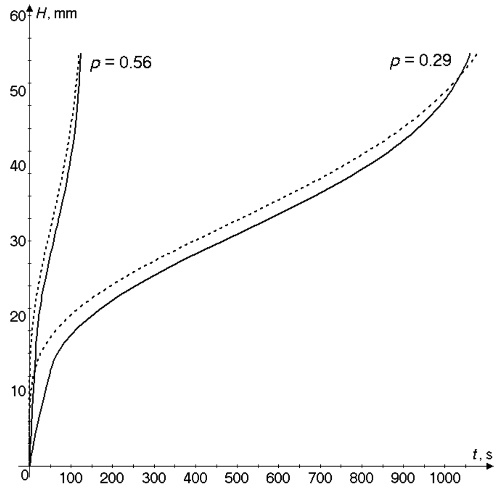

Fig. 9. Time dependence of the dome height *H*, mm, for aluminum alloy AA5083 calculated using ANSYS/Structural (solid lines) and by means of simplified analytical solutions (dashed lines) under different pressure, MPa, (indicated by the numbers near the curves) with $m = 0.29$, $K = 97.92$ MPa·s^m.

5. Conclusions

It is shown that the time of forming of a hemisphere made of Ti-6Al-4V titanium alloy at a constant pressure of an inert gas can be estimated with an error of no more than 1% by solving boundary value problems of the theory of creep, considering the pressure application in the first stage of forming the hemisphere, where the pressure increases from zero to a constant value and by including the presence of a die entry radius. In the magnesium alloy AZ31 and aluminum alloy AA5083 the error is no more than 3%, if only the die entry radius is considered, but not the presence of the first stage of forming where the inert gas pressure increases from zero to a constant value. Evidently, the accuracy of prediction is improved in including in the analysis the initial transient state where the inert gas pressure increases from zero to a pre-set constant value.

References

1. A.J. Barnes. J. Mater. Eng. Perform. 16 (4), 440 (2007). Crossref
2. J. Hedworth, M.J. Stowell. J. Mater. Sci. 6, 1061 (1971). Crossref
3. F. Jovane. Int. J. Mech. Sci. 10 (5), 403 (1968). Crossref
4. G.G. Cornfield, R.H. Johnson. Int. J. Mech. Sci. 12 (6), 479 (1970). Crossref
5. D.L. Holt. Int. J. Mech. Sci. 12, 491 (1970). Crossref
6. F.U. Enikeev, A.A. Kruglov. Int. J. Mech. Sci. 37 (5), 473 (1995). Crossref
7. G. Giuliano, S. Franchitti. Int. J. Mach. Tools Manuf. 48 (12-13), 1519 (2008). Crossref
8. F. Jarrar, R. Jafar, O. Tulupova, F. Enikeev, N. Al-Huniti. Mater. Sci. Forum, 838–839, 512 (2016). Crossref
9. S.A. Aksenov, I.Y. Zakhariev, I.V. Logashina. Letters on materials. 7 (1), 49 (2017). (in Russian) Crossref
10. S.A. Aksenov, V. Mikolaenko. Metals. 10 (10), 1353 (2020). Crossref
11. K.A. Padmanabhan, R.A. Vasin, F.U. Enikeev. Superplastic Flow. Springer-Verlag (2001) 363 p. Crossref
12. V.R. Ganieva, F.U. Enikeev, A.A. Kruglov. Mech. of Solids. 53 (2), 138 (2018). Crossref
13. O. Tulupova, V. Ganieva, A. Kruglov, F. Enikeev. Letters on materials. 7 (1), 68 (2017). (in Russian) Crossref
14. V. Ganieva, A. Kruglov, R. Lutfullin, O. Rudenko, F. Enikeev. IOP Conf. Ser.: Mater. Sci. and Eng. 447, 012050 (2018). Crossref
15. R.A. Vasin, F.U. Enikeev, M. Tokuda, R.V. Safiullin. Int. J. of Non-linear Mech. 35, 799 (2003). Crossref
16. V.R. Ganieva, O.P. Tulupova, F.U. Enikeev, A.A. Kruglov. Russian Eng. Res. 37 (5), 401 (2017). Crossref
17. A.A. Kruglov, O.P. Tulupova, N.V. Olimpieva, V.R. Ganieva, F.U. Enikeev. IOP Conf. Ser.: Mater. Sci. and Eng. 1008, 012050 (2020). Crossref
18. G.R. Murzina, V.R. Ganieva, A.A. Kruglov, F.U. Enikeev. Letters on materials. 11 (4s), 548 (2021). Crossref
19. O.P. Tulupova, V.R. Ganieva, A.A. Kruglov, F.U. Enikeev. IOP Conf. Ser.: Mater. Sci. and Eng. 447, 012039 (2018). Crossref
20. G. Dai, F. Jarrar, F. Ozturk, J. Sheikh-Ahmad, Z. Li. Open Access Metallurgy J. 9 (12), 1273 (2019). Crossref
21. G. Dai, F. Jarrar, F. Ozturk, J. Sheikh-Ahmad. Defect and Diffusion Forum. 385, 379 (2018). Crossref